frontiers | Frontiers in Physics

TYPE Original Research
PUBLISHED 09 January 2026
DOI 10.3389/fphy.2025.1729719

OPEN ACCESS

EDITED BY
Lev Shchur,
National Research University Higher School of Economics, Russia

REVIEWED BY
Yousef Azizi,
Independent Researcher, Zanjan, Iran
Atul Ray,
Madhav Institute of Technology and Science Gwalior, India

*CORRESPONDENCE
Ting Zhang,
zhangting0720@126.com,
zhangting0720@yau.edu.cn

RECEIVED 21 October 2025
REVISED 29 November 2025
ACCEPTED 03 December 2025
PUBLISHED 09 January 2026

CITATION
Zhang T (2026) Exact soliton solutions of the modified simplified Camassa–Holm and modified Benjamin–Bona–Mahony equations via the subsidiary ODE method .
Front. Phys. 13:1729719.
doi: 10.3389/fphy.2025.1729719

Exact soliton solutions of the modified simplified Camassa–Holm and modified Benjamin–Bona–Mahony equations via the subsidiary ODE method

Ting Zhang*

College of Mathematics and Computer Science, Yan'an University, Yan'an, Shaanxi, China

The main objective of this article is the analytical investigation of the simplified modified Camassa–Holm (SMCH) and the modified Benjamin–Bona–Mahony (BBM) equations. The SMCH equation plays an important role in modeling shallow-water wave dynamics, nonlinear dispersive phenomena, and the propagation of solitons in fluid mechanics. The BBM equation is frequently used to describe long surface gravity waves in nonlinear dispersive media and serves as a useful alternative to the standard Korteweg–de Vries (KdV) equation in mathematical physics. To construct exact analytical soliton solutions for these nonlinear models, the subsidiary ordinary differential equation (sub-ODE) method is employed. Through an appropriate wave transformation, the governing partial differential equations are reduced to nonlinear ordinary differential equations. Our mathematical technique yields several types of soliton wave shapes, including bright, dark, solitary, and periodic solitons. Bright solitons depict localized wave peaks, whereas dark solitons reflect intensity decreases against a continuous background. The resulting analytical solutions are represented in hyperbolic and trigonometric functions that exhibit complex nonlinear behaviors, such as periodic and singular patterns. These soliton structures exhibit the complex dynamics and stability of nonlinear waves propagating in dispersive mediums. The graphical demonstration of their propagation in three-dimensional, two-dimensional, and contour forms is presented for suitable parameter values.

KEYWORDS

bright soliton solutions, dark soliton solutions, exact soliton solutions, integrable systems, nonlinear evolution equations, nonlinear partial differential equations, periodic solutions, sub-ODE method

1 Introduction

The study of exact solutions for nonlinear partial differential equations (NLPDEs) is important for understanding nonlinear wave phenomena in several fields, including quantum mechanics, nonlinear optics, fluid mechanics, and plasma physics [1–5]. Nonlinear waves are essential for simulating shallow-water waves, electrical field propagation, acoustic–gravity waves, and hydromagnetic waves, along with other complex

physical systems [6–10]. Solitons are stable and confined wave structures that preserve geometry and energy throughout propagation despite nonlinearity and dispersion [11–15]. Bright solitons reflect isolated wave peaks, whereas dark solitons correspond to intensity decreases within a continuous background. Mixed solitons and singular solitons show the complexities in nonlinear wave dynamics [16–19]. Several analytical and computational approaches are being developed to address NLPDEs and generate soliton solutions. These include the *tanh*-function method, Jacobi elliptic function expansion, Hirota bilinear method, (G'/G)-expansion method, *sine* – *cosine* method, Exp-function method, Painlevé analysis, subsidiary ordinary differential equation (sub-ODE) method, variational iteration method, homotopy perturbation technique, Adomian decomposition method, and modified simple equation method [20–28]. These approaches yield explicit models for soliton solutions while also providing useful insights regarding the dynamics and stability of nonlinear waves over diverse media.

Research on nonlinear evolution equations has increasingly focused on Lie symmetries, optimal systems, and symmetry-based reduction techniques in order to obtain exact solutions and analyze nonlinear wave dynamics. Works on the Kadomtsev–Petviashvili (KP)–Benjamin–Bona–Mahony (BBM) and Zakharov–Kuznetsov (ZK)–BBM equations have presented optimal systems and group-invariant solutions that showcase complex structures and solution behaviors of multidimensional models [29, 30]. Furthermore, symmetry reductions are addressed for models such as the Korteweg–de Vries (KdV)–Burgers equation with appropriate dissipative mechanisms that are relevant in plasma environments, where the exact solutions provide insight into wave steepening and damping [31]. Works on one-dimensional (1D) gas dynamics under monochromatic radiation have extended the symmetry techniques to radiative hydrodynamics and sketched the role of Lie invariants in uncovering physically relevant wave patterns [32]. Similarly, in the case of the Gardner equation, studies have pointed out symmetry-based methods for constructing invariant solutions for nonlinear dispersive systems [33].

Various analyses of dissipative and acoustical wave equations are presented in many works, including the Zabolotskaya–Khokhlov equation, where the consideration of symmetry structures effectively reveals the underlying analytical forms of exact solutions that account for nonlinear acoustic propagation [34]. [35] also constructed invariant solutions of coupled Burgers equations, providing new insights into the soliton dynamics of multi-component systems. Symmetry reduction of the KP equation has provided new classes of exact solutions that are relevant in shallow-water wave theory and plasma physics [36]. The most recent works on the Broer–Kaup–Kupershmidt system illustrate how symmetries can be used to understand the interaction of solitons with conservation structures in shallow-water flows [37]. Beyond nonlinear mathematical physics, one finds modern imaging applications such as energy-resolved neutron tomography, in which advanced modeling links wave-based analytical tools to material characterization, thereby illustrating the growing interdisciplinary range of wave dynamics and transport analysis [38].

The simplified modified Camassa–Holm (SMCH) equation and the modified BBM (MBBM) equation are key models for analyzing nonlinear dispersive waves. The main point of the SMCH equation is that it is widely used to model shallow-water wave dynamics, soliton propagation in fluid systems, and nonlinear dispersive phenomena. The MBBM equation can be utilized to describe long surface gravity waves and serves as an alternative to the classical KdV equation [39–43]. Both models are applicable to thermodynamics and fluid mechanics, and they are widely employed in nonlinear optics and plasma physics, along with electromagnetic wave propagation. The sub-ODE method is an efficient analytical strategy for converting complex partial differential equations (PDEs) into simpler ordinary differential equations using proper wave transformations. This approach expresses traveling wave solutions as polynomials of sub-ODE solutions. Using the sub-ODE approach on the SMCH and MBBM equations yields a variety of precise solutions, including bright, dark, composite, and singular solitons. These solutions, which are frequently described as hyperbolic and trigonometric functions, exhibit complex nonlinear patterns and may be represented using two-dimensional (2D), three-dimensional (3D), and contour plots to highlight their stability and dynamics [44, 45].

The study of the soliton solutions for NLPDEs using contemporary analytical methods not only improves our understanding of nonlinear wave phenomena but also offers practical insights related to applications in optical fibers, fluid mechanics, plasma physics, and electromagnetic wave propagation. A systematic investigation into the structures of solitons within both the SMCH and MBBM equations reveals the richness of nonlinear dynamics and shows that modern mathematical techniques can be used to solve complex nonlinear evolution equations. The remainder of this article is organized as follows: Section 1 provides the introduction. Section 2 presents the results of the SMCH equation. Section 4 covers the extraction of soliton solutions for the modified BBM equation. Sections 3 and 5 describe the physical behavior of these solutions. Finally, Section 6 presents the conclusion.

2 Solutions of the SMCH equation

2.1 Mathematical analysis of the sub-ODE method

The emphasis in this article on one-dimensional equations represents a basic and strategic approach to method validation, given the current trend of research into higher-dimensional models. Reductions such as the SMCH and modified BBM equations represent essential one-dimensional benchmark cases in nonlinear wave theory. Such models arise naturally from multi-dimensional systems in fluid mechanics and plasma physics using standard methods of dimensional reduction. The main emphasis of this article is on the development and rigorous validation of the generalized sub-ODE method, and 1D settings represent the established testing ground for analytical correctness, numerical stability, and computational accuracy. Solution families U_1–U_{12} obtained in this article are intrinsically of mathematical interest, and more importantly, they represent a starting point for extensions to higher-dimensional analogs, such as the Camassa–Holm–Kadomtsev–Petviashvili-type models and two-dimensional variants of BBM equations. A gradual approach from one-dimensional validation to higher-dimensional applications is

a step-by-step research strategy that assures robust development of the method before moving on to more complex geometrical settings.

We assume that the NLPDE is constructed for the function $g = g(x,t)$, where x and t are the spatial and temporal variables, respectively. This assumption allows us to use analytical approaches to find precise or approximate solutions for the NLPDE:

$$Q\left(g, g_x, g_t, g_{xx}, g_{xt}, g_{tt}, \ldots\right) = 0, \tag{1}$$

where Q denotes a polynomial containing the function g and its greatest order partial derivative. The traveling wave transformation is used to convert the nonlinear differential equation into an ordinary differential equation:

$$g(x,t) = g(\xi), \qquad \xi = x \pm \omega t, \tag{2}$$

where ξ shows the transformation. In this case, $\omega \neq 0$ is a constant to be determined later. Substituting Equation 1 into Equation 2 yields the ordinary differential equation (ODE) for further investigation:

$$H\left(g, g', g'', g''', g^{(4)}, \ldots\right) = 0, \tag{3}$$

where

$$g = g(\xi), \qquad g' = \frac{dg}{d\xi}, \qquad g'' = \frac{d^2 g}{d\xi^2}, \ldots.$$

The solution of Equation 3 is provided as follows, which is used to construct explicit forms of the traveling wave solutions:

$$g(\xi) = \sum_{i=0}^{N} a_i \psi^i(\xi), \qquad a_i \neq 0, \tag{4}$$

where a_i $(i = 0, 1, 2, \ldots, N)$ signifies the constants to be calculated. $\psi(\xi)$ represents the solution of the following equation:

$$\psi'^2 = h_0 + h_2 \psi^2 + h_4 \psi^4, \tag{5}$$

where h_0, h_2 and h_4 are real constants.

2.2 Description of the SMCH equation

Camassa and Holm [22] derived the CH equation for shallow-water waves in 1993. It has an integrable bi-Hamiltonian structure. The SMCH equation is written as follows:

$$U_t + 2\alpha U_x - U_{xxt} + \beta U^2 U_x = 0, \tag{6}$$

where $\alpha \in \mathbb{R}$; $\beta > 0$ and $U(x,t)$ represents the fluid velocity in the x-direction. Using wave transformation, we obtain

$$U(x,t) = U(\xi), \qquad \xi = x - \omega t. \tag{7}$$

Substituting Equation 7 into Equation 6 converts the original PDE into an ODE in terms of the traveling wave variable. This reduction simplifies the problem, making it easier to evaluate and create clear solutions.

$$-\omega U' + 2\alpha U' + \omega U''' + \beta U^2 U' = 0. \tag{8}$$

To minimize the order of the differential equation, we integrate Equation 8 with respect to ξ and simplify the resultant expression. This phase eliminates the highest-order derivative and inserts an integration constant, which may be computed later using boundary or beginning conditions.

$$\omega U - 2\alpha U - \omega U'' - \frac{\beta}{3} U^3 = 0. \tag{9}$$

2.3 Exact solutions of the SMCH equation

We use the balancing principle to determine the explicit form of the traveling wave solution. We first substitute the ansatz $U(\xi) = \psi(\xi)^N$, where $\psi = \psi(\xi)$ is to be determined and N is a positive integer, into the governing equation. The highest-order derivative U'' and the highest-order nonlinear term U^3 are the dominant terms. Substituting the ansatz, U'' yields a power of ψ^{N+2}, whereas the nonlinear term U^3 yields a power of ψ^{3N}. For a non-trivial solution to exist, these dominant terms must be balanced. Thus, it follows that the powers of ψ must be equal. This produces an algebraic equation $N + 2 = 3N$. If we solve the equation, we obtain $2 = 2N$ and, ultimately, $N = 1$. This supports that the solution of $U(\xi)$ must be written as $U(\xi) = a_0 + a_1 \psi(\xi)$.

Employing the balancing method for the terms U'' and U^3 in Equation 9 yields $N = 1$. To balance the nonlinear variable U^3 and the highest-order derivative term U'', the maximum power of $\psi(\xi)$ in the proposed solution must be 1. As a result, Equation 9 enables a solution with just the first-order terms of $\psi(\xi)$

$$U(\xi) = a_0 + a_1 \psi(\xi), \tag{10}$$

where a_0 and a_1 are arbitrary constants that will be determined later and $\psi(\xi)$ is the solution to the related elliptic differential equation. The function $\psi(\xi)$ controls the amplitude and periodic behavior of the wave in the soliton solution, establishing its general structure as

$$\psi'' = h_2 \psi + 2h_4 \psi^3, \qquad (\psi')^2 = h_0 + h_2 \psi^2 + h_4 \psi^4, \tag{11}$$

where h_0, h_2, and h_4 are real constants. Substituting Equation 10 and Equation 11 into Equation 12 creates a new equation that relates these constants through algebraic expressions. This substitution reduces the nonlinear components and prepares the problem for an analytical approach.

$$\begin{aligned} &a_0\omega - 2\alpha a_0 - \frac{1}{3}\beta a_0^3 + a_1\omega\psi - 2\alpha a_1\psi - \beta a_0^2 a_1\psi - a_1 h_2\omega\psi - a_0 a_1^2\beta\psi^2 \\ &\quad - \frac{1}{3}\beta a_1^3\psi^3 - 2a_1 h_4\omega\psi^3 = 0. \end{aligned} \tag{12}$$

To verify that the equation holds true for all values of ψ, the coefficients of each power of ψ are equated to 0. As a result, a set of algebraic equations is obtained, which enables the determination of the unknown constants such as a_0, a_1, h_0, h_2, and h_4.

$$\begin{aligned} \psi^0&: \quad a_0\omega - 2\alpha a_0 - \frac{1}{3}\beta a_0^3 = 0, \\ \psi^1&: \quad a_1\omega - 2\alpha a_1 - a_0^2 a_1\beta - a_1 h_2\omega = 0, \\ \psi^2&: \quad -a_0 a_1^2\beta = 0, \\ \psi^3&: \quad -\frac{1}{3}\beta a_1^3 - 2a_1 h_4\omega = 0. \end{aligned}$$

The solution to these algebraic equations will yield the exact value of the unknown constants, and such constants are necessary for forming the exact traveling wave solutions. These constants determine the type and number of solitons generated by the nonlinear equation, including bright, dark, and singular solutions.

$$a_0 = 0, \quad \omega = -\frac{2\alpha}{h_2 - 1}, \quad a_1 = \pm 2\sqrt{\frac{3\alpha h_4}{\beta h_2 - \beta}}. \tag{13}$$

The solution to Equation 11 may be represented as follows by demonstrating the relationship between Jacobi elliptic functions and

TABLE 1 Analysis of Jacobi elliptic functions and their limiting forms.

Function	$j \to 1$	$j \to 0$	Function	$j \to 1$	$j \to 0$	Function	$j \to 1$	$j \to 0$
sn (ξ, j)	tanh (ξ)	sin (ξ)	ds (ξ, j)	csch (ξ)	csc (ξ)	cn (ξ, j)	sech (ξ)	cos (ξ)
dn (ξ, j)	sech (ξ)	1	sd (ξ, j)	sinh (ξ)	sin (ξ)	ns (ξ, j)	coth (ξ)	csc (ξ)
nc (ξ, j)	cosh (ξ)	sec (ξ)	cs (ξ, j)	csch (ξ)	cot (ξ)	cd (ξ, j)	1	cos (ξ)

their limiting forms. When the modulus j approaches 1 or 0, these functions become hyperbolic and trigonometric.

Table 1 describes Jacobi elliptic functions and their limiting forms, which are essential for generating soliton solutions in nonlinear differential equations. The table depicts the behavior of each function (sn, cn, dn, ds, sd, ns, nc, cs, and cd) as the modulus $j \to 1$ and $j \to 0$. When $j \to 1$, the functions decrease to hyperbolic functions (tanh, sech, sinh, coth, etc.), and they depict localized soliton-like waves. When $j \to 0$, they reduce to trigonometric functions (sin, cos, sec, csc, cot, etc.), and they characterize periodic waves. This shows that, depending on the value of j, a single Jacobi function may describe both soliton and periodic wave solutions, making it particularly helpful for evaluating traveling wave solutions and soliton structures in nonlinear wave equations.

2.3.1 Case 1

We assume that $h_0 = v^2 D^2$, $h_2 = -v^2(1 + j^2)$, and $h_4 = \frac{v^2 j^2}{D^2}$. Here, v and D are the wave velocity and the amplitude of the wave, respectively, and $0 \le j \le 1$ is the Jacobi elliptic function modulus. The solution of Equation 11 is as follows:

$$\psi(\xi) = D\,\mathrm{sn}\,(v\xi, j). \tag{14}$$

The exact solution of Equation 8 is mathematically represented below, where the parameters meet the given requirements.

$$U_1(\xi) = \pm 2vj\sqrt{-\frac{3\alpha}{\beta\left(v^2 + v^2 j^2 + 1\right)}}\,\mathrm{sn}\,(v\xi, j), \quad \omega = \frac{2\alpha}{v^2\left(1 + j^2\right) + 1}. \tag{15}$$

In the limiting case, as $j \to 1$, the solution of Equation 11 simplifies to a hyperbolic shape, representing a confined solitary wave. This limit illustrates the transition from periodic Jacobi elliptic functions to solitary wave structures, stressing the solution's physical relevance in the context of nonlinear wave propagation.

$$U_1(\xi) = \pm 2v\sqrt{-\frac{3\alpha}{\beta\left(2v^2 + 1\right)}}\,\tanh(\xi), \xi = x - \frac{2\alpha t}{2v^2 + 1}. \tag{16}$$

2.3.2 Case 2

We assume a certain value of $h_0 = v^2 D^2(1 - j^2)$, $h_2 = -v^2(2j^2 - 1)$, and $h_4 = -\frac{v^2 j^2}{D^2}$. Equation 11 admits the following exact solution, which depends on the Jacobi elliptic functions and characterizes the wave profile for the system under consideration.

$$\psi(\xi) = D\,\mathrm{cn}\,(v\xi, j). \tag{17}$$

The solution of Equation 8 can be written as follows, illustrating the system behavior under the specified conditions:

$$U_2(\xi) = \pm 2vj\sqrt{\frac{3\alpha}{\beta\left(2v^2 j^2 - v^2 + 1\right)}}\,\mathrm{sn}\,(v\xi, j), \quad \omega = \frac{2\alpha}{v^2\left(2j^2 - 1\right) + 1}. \tag{18}$$

As $j \to 1$, the outcome becomes hyperbolic, corresponding to a specific soliton with a sharp peak and finite width. This shows the creation of a single wave in the structure of the system.

$$\xi = x - \frac{2\alpha t}{v^2 + 1}, \quad U_2(\xi) = \pm 2v\sqrt{\frac{3\alpha}{\beta\left(v^2 + 1\right)}}\,\mathrm{sech}\,(\xi). \tag{19}$$

2.3.3 Case 3

We assume that $h_0 = -v^2 D^2(1 - j^2)$, $h_2 = v^2(2 - j^2)$, and $h_4 = -\frac{v^2}{D^2}$. Based on Equation 11, the solution captures the system's nonlinear properties and can represent several solitons depending on the parameters used.

$$\psi(\xi) = D\,\mathrm{dn}\,(v\xi, j). \tag{20}$$

The solution of Equation 8 can be stated as follows, demonstrating the system behavior under the required conditions:

$$U_3(\xi) = \pm 2v\sqrt{\frac{3\alpha}{\beta\left(v^2 j^2 - 2v^2 + 1\right)}}\,\mathrm{dn}\,(v\xi, j), \omega = -\frac{2\alpha}{v^2\left(2 - j^2\right) - 1}. \tag{21}$$

As $j \to 1$, the outcome becomes hyperbolic, representing a particular soliton with a sharp peak and finite width. This demonstrates the formation of a single wave within the system's structure.

$$U_3(\xi) = \pm 2\,v\sqrt{\frac{3\alpha}{\beta\left(-v^2 + 1\right)}}\,\mathrm{sech}\,(\xi), \quad \xi = x + \frac{2\alpha t}{v^2 - 1}. \tag{22}$$

2.3.4 Case 4

We assume that $h_0 = v^2 D^2 j^2$, $h_2 = -v^2(1 + j^2)$, and $h_4 = \frac{v^2}{D^2}$. The solution to Equation 11 shows how the wave profile evolves over time. This solution captures the system's nonlinear features and can represent a variety of solitons depending on the parameters used.

$$\psi(\xi) = D\,\mathrm{ns}\,(v\xi, j) = \frac{D}{\mathrm{sn}\,(v\xi, j)}. \tag{23}$$

The solution of Equation 8 can be expressed as follows, illustrating the system behavior under suitable conditions:

$$U_4(\xi) = \pm 2\,v\sqrt{\frac{3\alpha}{-\beta\left(v^2 j^2 + v^2 + 1\right)}}\,\mathrm{ns}\,(v\xi, j), \quad \omega = \frac{2\alpha}{v^2\left(1 + j^2\right) + 1}. \tag{24}$$

As $j \to 1$, the result becomes hyperbolic, indicating a specific soliton with a sharp peak and finite width. This shows how a single wave forms within the system's structure.

$$U_4(\xi) = \pm 2\nu \sqrt{\frac{3\alpha}{-\beta(2\nu^2+1)}} \coth(\xi), \quad \xi = x - \frac{2\alpha t}{2\nu^2+1}. \tag{25}$$

2.3.5 Case 5

We assume that $h_0 = -\nu^2 D^2 j^2$, $h_2 = \nu^2(2j^2-1)$, and $h_4 = \nu^2 \frac{1-j^2}{D^2}$. From Equation 11, the solution captures the system's nonlinear properties and can represent several solitons depending on the parameters used.

$$\psi(\xi) = D\,\mathrm{nc}(\nu\xi, j) = \frac{D}{\mathrm{cn}(\nu\xi, j)}. \tag{26}$$

The solution to Equation 8 is as follows, showing the behavior of the system under the appropriate conditions:

$$U_5(\xi) = \pm 2\nu \sqrt{\frac{3\alpha(1-j^2)}{-\beta(\nu^2 - 2\nu^2 j^2 + 1)}}\,\mathrm{nc}(\nu\xi, j), \quad \omega = \frac{-2\alpha}{\nu^2(2j^2-1)-1}. \tag{27}$$

As $j \to 0$, the result becomes hyperbolic, suggesting a unique soliton with a sharp peak and finite width. This illustrates how a single wave forms within the system's structure.

$$U_5(\xi) = \pm 2\nu \sqrt{\frac{3\alpha}{-\beta(\nu^2+1)}}\,\sec(\xi), \xi = x + \frac{2\alpha t}{2\nu^2+1}. \tag{28}$$

2.3.6 Case 6

We assume that $h_0 = -\nu^3 D^2$, $h_2 = \nu^2(2-j^2)$, and $h_4 = -\frac{\nu^2(1-j^2)}{D^3}$. The solution of Equation 11 demonstrates how the wave profile varies over time. This solution represents the system's nonlinear features and can represent a variety of solitons based on the parameters used.

$$\phi(\xi) = D\,\mathrm{nd}(\nu\xi, j) = \frac{D}{\mathrm{dn}(\nu\xi, j)}. \tag{29}$$

The solution of Equation 8 is as follows, displaying the system behavior under the required conditions.

$$U_6(\xi) = \pm 2\nu \sqrt{\frac{3\alpha(1-j^2)}{\beta(\nu^2 j^2 - 2\nu^2 + 1)}}\,\mathrm{nd}(\nu\xi, j), \quad \omega = -\frac{2\alpha}{\nu^2(2-j^2)-1}. \tag{30}$$

2.3.7 Case 7

We assume that $h_0 = \nu^2 D^2$, $h_2 = \nu^2(2-j^2)$, and $h_4 = \frac{\nu^2(1-j^2)}{D^2}$. Based on Equation 11, the solution depicts the system's nonlinear properties and can represent several solitons depending on the parameters employed.

$$\psi(\xi) = D\,\mathrm{sc}(\nu\xi, j) = \frac{D\,\mathrm{sn}(\nu\xi, j)}{\mathrm{cn}(\nu\xi, j)}. \tag{31}$$

The solution of Equation 8 is shown below, demonstrating the system behavior under specific conditions.

$$j_7(\xi) = \pm 2\nu \sqrt{\frac{3\alpha(1-j^2)}{-\beta(\nu^2 j^2 - 2\nu^2 + 1)}}\,\mathrm{sc}(\nu\xi, j), \quad \omega = -\frac{2\alpha}{\nu^2(2-j^2)-1}. \tag{32}$$

As $j \to 0$, the result becomes hyperbolic, indicating a single soliton with a sharp peak and finite width. This demonstrates the development of a single wave within the system's internal structure.

$$U_7(\xi) = \pm 2\nu \sqrt{\frac{3\alpha}{-\beta(-2j^2+1)}}\,\tan(\xi), \quad \xi = x + \frac{2\alpha t}{2\nu^2-1}. \tag{33}$$

2.3.8 Case 8

We assume that $h_0 = \nu^2 D^2$, $h_2 = \nu^2(2j^2-1)$, and $h_4 = -\frac{\nu^2 j^2(1-j^2)}{D^2}$. The solution of Equation 11 illustrates how the wave profile varies over time. This solution displays the system's nonlinear features and can represent a variety of solitons depending on the parameters used.

$$\psi(\xi) = D\,\mathrm{sd}(\nu\xi, j) = \frac{D\,\mathrm{sn}(\nu\xi, j)}{\mathrm{dn}(\nu\xi, j)}. \tag{34}$$

The solution of Equation 8 is provided below, exhibiting the system's behavior under the given conditions.

$$U_8(\xi) = \pm 2\nu j \sqrt{\frac{3\alpha(1-j^2)}{\beta(\nu^2 - 2\nu^2 j^2 + 1)}}\,\mathrm{sd}(\nu\xi, j), \quad \omega = -\frac{2\alpha}{\nu^2(2j^2-1)-1}. \tag{35}$$

2.3.9 Case 9

We assume that $h_0 = \nu^2(1-j^2)$, $h_2 = \nu^2(2-j^2)D^2$, and $h_4 = \frac{\nu^2}{D^2}$. Based on Equation 11, the solution highlights the system's nonlinear properties and can depict several solitons depending on the parameters used.

$$\psi(\xi) = D\,\mathrm{cs}(\nu\xi, j) = \frac{D\,\mathrm{cn}(\nu\xi, j)}{\mathrm{sn}(\nu\xi, j)}. \tag{36}$$

The solution of Equation 8 is provided below, exhibiting the system's behavior under specified conditions.

$$U_9(\xi) = \pm 2\nu \sqrt{\frac{3\alpha}{-\beta(\nu^2 j^2 - 2\nu^2 + 1)}}\,\mathrm{cs}(\nu\xi, j), \quad \omega = -\frac{2\alpha}{\nu^2(2-j^2)-1}. \tag{37}$$

As j approaches 0, the result becomes hyperbolic, indicating a single soliton with a sharp peak and finite width. This demonstrates the formation of a single wave within the system's internal structure.

$$\xi = x + \frac{2\alpha t}{2\nu^2-1}, \quad U_9(\xi) = \pm 2\nu \sqrt{\frac{3\alpha}{-\beta(-2\nu^2+1)}}\,\mathrm{csch}(\xi). \tag{38}$$

2.3.10 Case 10

We assume that $h_0 = \nu^2 D^2$, $h_2 = -\nu^2(1+j^2)$, and $h_4 = \frac{\nu^2 j^2}{D^3}$. The solution of Equation 11 demonstrates how the wave profile varies over time. This solution emphasizes the system's nonlinear features and can represent a variety of solitons depending on the parameters used.

$$\psi(\xi) = D\,\mathrm{cd}(\nu\xi, j) = \frac{D\,\mathrm{cn}(\nu\xi, j)}{\mathrm{dn}(\nu\xi, j)}. \tag{39}$$

The solution of Equation 8 is provided below, exhibiting the system's behavior under certain conditions.

$$U_{10}(\xi) = \pm 2\nu j \sqrt{\frac{3\alpha}{-\beta(\nu^2 j^2 + \nu^2 + 1)}}\,\mathrm{cd}(\nu\xi, j), \quad \omega = \frac{2\alpha t}{\nu^2(1+j^2)+1}. \tag{40}$$

2.3.11 Case 11

We assume that $h_0 = -v^2j^2(1-j^2)$, $h_2 = v^2(2j^2-1)$. Finally, $h_4 = \frac{v^2}{D^2}$. The solution of Equation 11 illustrates how the wave profile varies over time. This solution highlights the system's nonlinear features and can represent a variety of solitons depending on the variables used.

$$\psi(\xi) = D\,\mathrm{ds}(v\xi, j) = \frac{D\,\mathrm{dn}(v\xi, j)}{\mathrm{sn}(v\xi, j)}. \tag{41}$$

The following solution of Equation 8 demonstrates the system's behavior under the provided conditions.

$$U_{11}(\xi) = \pm 2v\sqrt{\frac{3\alpha}{-\beta\left(v^2 - v^2j^2 + 1\right)}}\,\mathrm{ds}(v\xi, j), \quad \omega = \frac{2\alpha t}{v^2\left(2j^2-1\right) - 1}. \tag{42}$$

As $j \to 1$, the result turns hyperbolic, suggesting a single soliton with a sharp peak and finite width. This occurs when a single wave emerges within the system's underlying structure.

$$\xi = x - \frac{2\alpha t}{2v^2+1}, \quad U_{11}(\xi) = \pm 2v\sqrt{\frac{3\alpha}{-\beta\left(v^2+1\right)}}\,\mathrm{csch}(\xi). \tag{43}$$

2.3.12 Case 12

We suppose that $h_0 = v^2j^2D^2$, $h_2 = -v^2(j^2+1)$, and $h_4 = \frac{v^2}{D^2}$. The solution of Equation 11 shows how the wave profile changes with time. This solution emphasizes the system's nonlinear properties and can represent several solitons based on the parameters used.

$$\psi(\xi) = D\,\mathrm{dc}(v\xi, j) = \frac{D\,\mathrm{dn}(v\xi, j)}{\mathrm{sn}(v\xi, j)}. \tag{44}$$

The solution of Equation 8 is provided below, exhibiting the system's response under the given circumstances.

$$U_{12}(\xi) = \pm 2v\sqrt{\frac{3\alpha}{-\beta\left(v^2j^2 + v^2 + 1\right)}}\,\mathrm{csch}(\xi), \quad \omega = \frac{2\alpha t}{v^2\left(j^2+1\right) + 1}. \tag{45}$$

3 Physical interpretation of solutions under the SMCH equation

These graphs illustrate a clear representation of the different solitary wave solutions obtained for the considered SMCH equation. The dark soliton solution obtained from Equation 16 and plotted in Figure 1 represents a stable density dip traveling over a continuous background. By using parameters $v = 1.5$, $j = 1$, $\alpha = 0.1$, and $\beta = 0.5$, this structure models phenomena such as pressure depressions in compressible fluids or voids in nonlinear lattices, where the parameters dictate the depth and stability of the propagating trough. Bright soliton solutions are shown in Figures 2, 3 for Equations 19, 22, respectively, which manifest as localized, particle-like humps of elevated energy. These structures, specifically with the modulating parameter, as shown in Figure 2, are fundamental for modeling localized excitations such as pressure peaks in shallow water or intense pulses in elastic rods.

In this section, Maple 18 is utilized to generate 3D, 2D, and contour graphs of traveling wave solutions for the SMCH equation. Figure 1 shows that the series of solutions is extended with the inclusion of singular and periodic wave modes, which result from the nonlinearity of the SMCH model. The implementation of Equation 25 in Figure 4 shows a singular soliton with its characteristic unbounded and sharp peak that points to a scenario of wave-breaking or hydraulic jump in the case of fluid dynamics; here, the choice of $j = 0$ is crucial for the observation of the non-analytic characteristic. Figure 5 shows a periodic singular soliton, derived from Equation 28; the periodicity of the singularity indicates that the system frequently undergoes shock formation. Figure 6 (from Equation 33) reveals a non-singular wave that is purely periodic and has similarities to oscillatory forms within confined domains. The singular soliton in Figure 7 (from Equation 38), on the other hand, not only suggests but also emphasizes the possible occurrence of highly localized, intense energy concentrations that might be the precursor of rogue waves in a complex medium.

The multi-perspective plotting strategy using 3D, 2D, and contour views physically elucidates the features of the SMCH equation step by step. The 3D surface plots clearly demonstrate the strong localization in the space and the stability over time of the soliton amplitude. The 2D line graphs corresponding to the 3D surface plots provide a detailed view of the wave's profile at the moment and its invariance in translation over the spatial domain. The contour plots clearly delineate the mapping of intensity lines and the pathways of energy propagation, thus providing important insights into the collisionless nature and interaction capabilities of solitons. The use of different plots not only illustrates various mathematical solutions but also highlights the rich physics and the wide range of wave morphologies that can be observed and are governed by the SMCH equation under the given parameter conditions.

4 Extraction of soliton solutions for the modified BBM equation

4.1 Description of the modified BBM equation

The $(1+1)$-dimensional nonlinear dispersed modified BBM (Equation 11) is an important model for studying weakly nonlinear long waves in dispersive media. This equation reflects the equilibrium between nonlinearity and dispersion, which allows the existence and propagation of a wide range of solitary wave solutions. The result is as follows:

$$u_t + u_x - \alpha u^2 u_x + u_{xxx} = 0, \tag{46}$$

where α represents a non-zero real constant. This equation was originally formulated to represent long surface waves in a nonlinear dispersive medium. It may also describe acoustic–gravity waves in compressible fluids, hydromagnetic waves in cold plasmas, and acoustic waves in inharmonic crystals. We know that from the previous section, the traveling wave transformation is stated as follows:

$$U(x,t) = U(\xi), \qquad \xi = x - \omega t. \tag{47}$$

Using the chain rule, $U_t = -\omega U'$, $U_x = U'$, $U_{xxx} = U'''$. Substituting Equation 47 into Equation 46 yields a nonlinear ODE incorporating

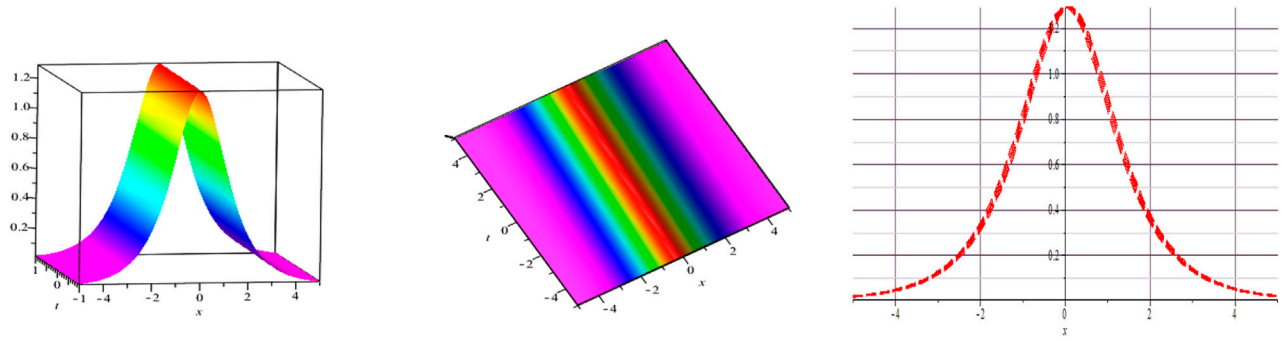

FIGURE 1
Three different graphical representations, namely, 3D surface (left panel), contour plot (middle panel), and 2D profile (right panel), of the solution of Equation 16 for the parameter values $v = 1.5$, $j = 1$, $\alpha = 0.1$, and $\beta = 0.5$. These graphs describe the structure of a dark optical soliton under the specified constraints.

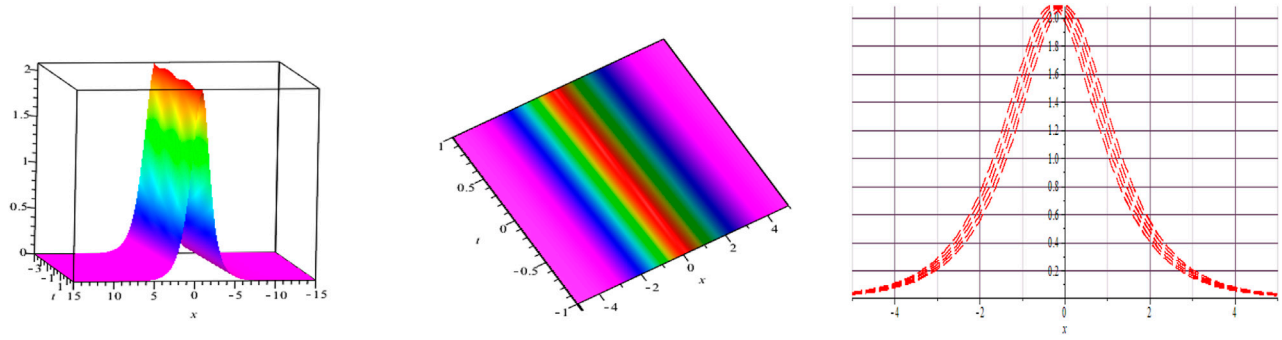

FIGURE 2
Three different graphical representations, namely, 3D surface (left panel), contour plot (middle panel), and 2D profile (right panel), of the solution of Equation 19 for the parameter values $v = 1.5$, $j = 1$, $\alpha = 0.1$, $\beta = 0.5$, and $\chi = 0.1$. These graphs describe the structure of a bright soliton under the specified constraints.

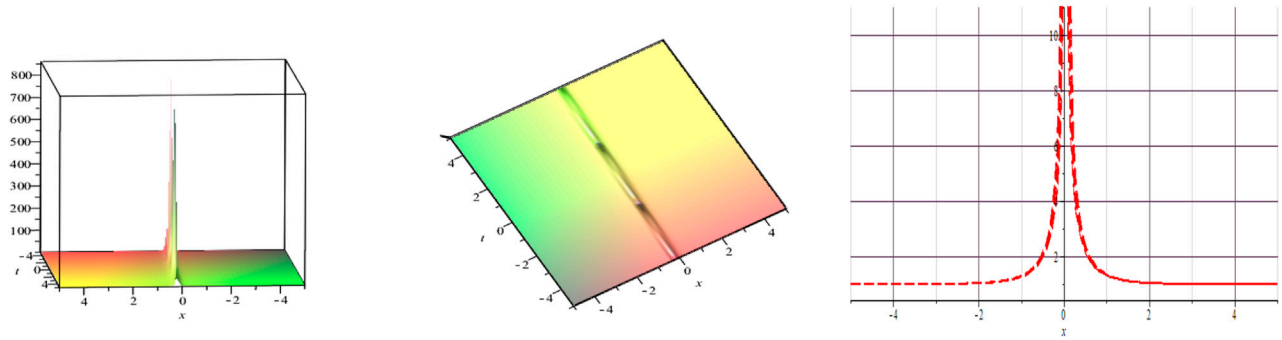

FIGURE 3
Three different graphical representations, namely, 3D surface (left panel), contour plot (middle panel), and 2D profile (right panel), of the solution of Equation 22 for the parameter values $v = 1.5$, $j = 1$, $\alpha = 0.1$, and $\beta = 0.5$. These graphs describe the structure of a bright soliton under the specified constraints.

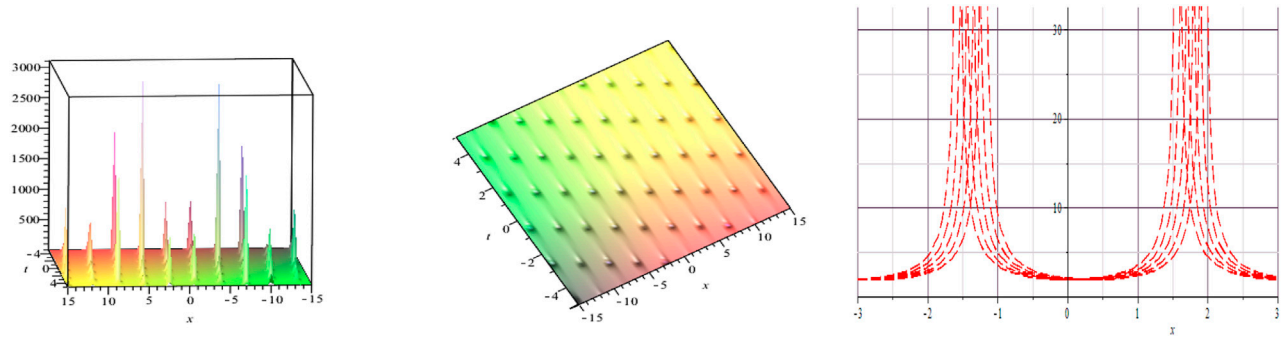

FIGURE 4
Three different graphical representations, namely, 3D surface (left panel), contour plot (middle panel), and 2D profile (right panel), of the solution of Equation 25 for the parameter values $v = 1.5$, $j = 0$, $\alpha = 0.1$, and $\beta = 0.5$. These graphs describe the unique soliton structure under the specified constraints.

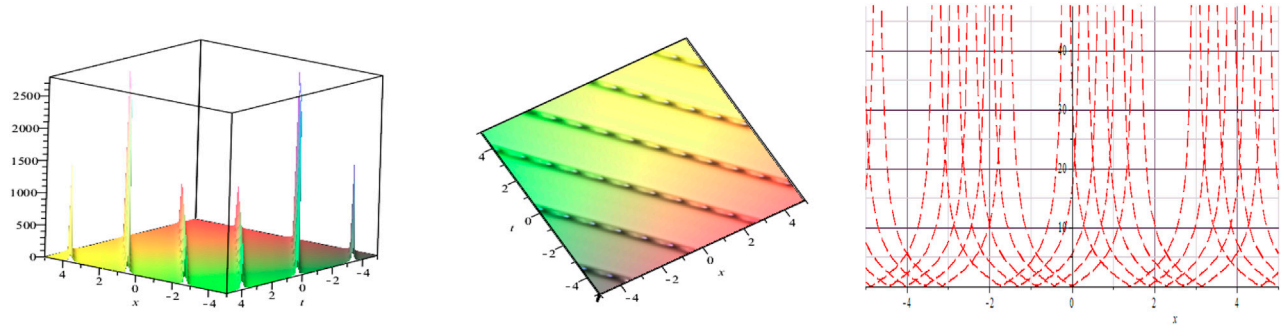

FIGURE 5
Three different graphical representations, namely, 3D surface (left panel), contour plot (middle panel), and 2D profile (right panel), of the solution of Equation 28 for the parameter values $v = 1.5$, $j = 0$, $\alpha = 0.1$, and $\beta = 0.5$. These graphs describe the periodic singular solitons under the specified constraints.

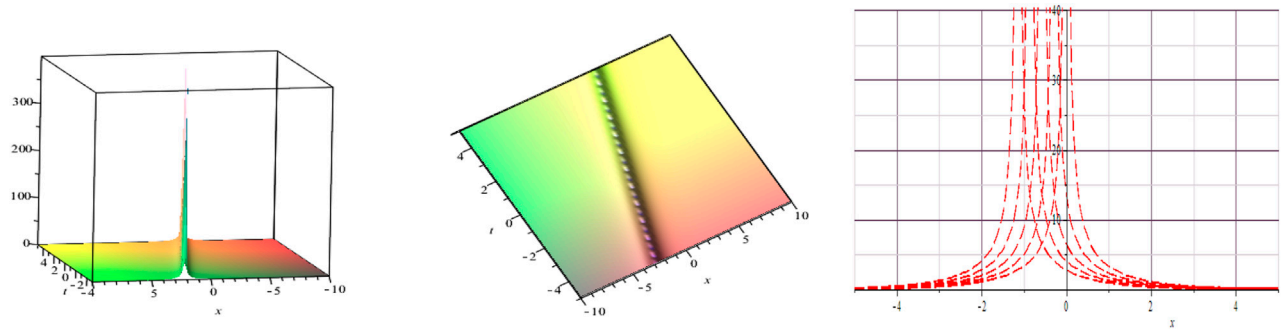

FIGURE 6
Three different graphical representations, namely, 3D surface (left panel), contour plot (middle panel), and 2D profile (right panel), of the solution of Equation 33 for the parameter values $v = 1.5$, $j = 0$, $\alpha = 0.1$, and $\beta = 0.5$. These graphs describe the periodic soliton under the specified constraints.

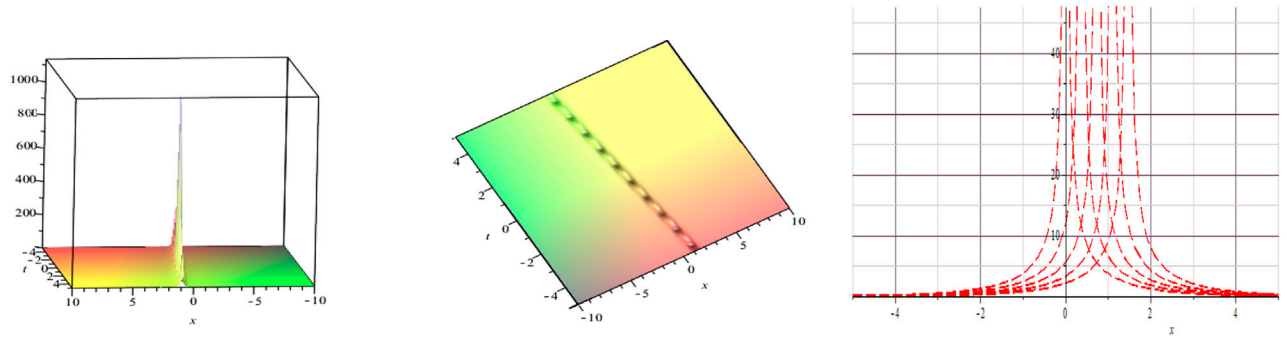

FIGURE 7
Three different graphical representations, namely, 3D surface (left panel), contour plot (middle panel), and 2D profile (right panel), of the solution of Equation 38 for the parameter values $v = 1.5$, $j = 1$, $\alpha = 0.1$, and $\beta = 0.5$. These graphs describe a singular optical soliton under the specified constraints.

U and its derivatives. This transformation essentially lowers the original partial differential equation to an ODE, which simplifies wave profile analysis. The resultant equation is as follows:

$$(1-\omega)\,U' - \alpha\,U^2U' + U''' = 0. \tag{48}$$

Combining Equation 48 with respect to ξ while allowing the constant integration to be 0 for simplicity yields a simplified equation. This technique significantly reduces the order of the differential equation, making it easier to derive exact traveling wave solutions. The integrated equation reflects the balance among nonlinear and dispersive effects that exist in the system, which is necessary for understanding soliton structures.

$$(1-\omega)\,U - \frac{\alpha}{3}U^3 + U'' = 0. \tag{49}$$

4.2 Exact solution of the modified BBM equation

Using the balance concept from Equation 49, we obtain $n = 1$. This step is critical for developing precise traveling wave solutions and guarantees that the nonlinear and dispersive terms are correctly balanced.

$$U(\xi) = a_0 + a_1\,\psi(\xi), \tag{50}$$

where a_0 and a_1 are arbitrary constants and $\psi(\xi)$ satisfies an elliptic differential equation. This approach allows for the generation of precise traveling wave solutions by selecting the function $\psi(\xi)$ to satisfy the governing nonlinear equation.

$$(\psi')^2 = h_0 + h_2\,\psi^2 + h_4\,\psi^4, \qquad \psi'' = h_2\,\psi + 2h_4\,\psi^3, \tag{51}$$

where h_0, h_2, and h_4 are real constants. Substituting Equation 50 and Equation 51 into Equation 49 yields an equation in terms of $\psi(\xi)$ and its powers. This technique allows us to determine the unknown coefficient h_0, h_2, h_4 consistently by comparing the coefficients of similar powers of $\psi(\xi)$, eventually leading to exact solutions of the nonlinear equation

$$a_0 - a_0\omega - \frac{1}{3}\alpha a_0^3 + a_1\psi - a_1\omega\psi - a_0^2a_1\psi + a_1h_2\psi - \alpha a_0a_1^2\psi^2 - \frac{1}{3}\alpha a_1^3\psi^3 + 2a_1h_4\psi^3 = 0. \tag{52}$$

A set of equations involving algebra can be obtained by equating every coefficient of power of ψ to 0. These equations provide information on the unknown constants within the solution. Solving them yields the precise analytical structure of the traveling wave solution.

$$\begin{aligned}
\psi^0&: \quad a_0 - a_0\omega - \frac{1}{3}\alpha a_0^3 = 0,\\
\psi^1&: \quad a_1 - a_1\omega - a_0^2a_1 + a_1h_2 = 0,\\
\psi^2&: \quad -\alpha a_0a_1^2 = 0,\\
\psi^3&: \quad 2a_1h_4 - \frac{1}{3}\alpha a_1^3 = 0.
\end{aligned}$$

Solving the above algebraic equations yields the values of unknown constants, thereby allowing us to construct the explicit form of the traveling wave solution.

$$a_0 = 0, \quad \omega = 1 + h_2, \quad a_1 = \pm\sqrt{\frac{6h_4}{\alpha}}. \tag{53}$$

The exact solution of Equation 51 is provided in the following section, illustrating the traveling wave form that satisfies the nonlinear equation.

4.2.1 Case 1

We assume that $h_0 = v^2C^2$, $h_2 = -v^2(1+m^2)$, and $h_4 = \frac{v^2m^2}{C^2}$. Here, v and C are nonzero real constants, while $0 \le m \le 1$ is the Jacobi elliptic functions' modulus. The result of Equation 51 is as follows:

$$\psi(\xi) = C\,\mathrm{sn}(v\xi, m). \tag{54}$$

The specific solution of Equation 48 may be written as follows, which offers insight into the behavior of the structure under consideration.

$$\omega = 1 - v^2\left(1+m^2\right), \tag{55}$$

$$U_1(\xi) = \pm vm\sqrt{\frac{6}{\alpha}}\,\mathrm{sn}(v\xi, m). \tag{56}$$

As $m \to 1$, the outcome reveals the system's limiting behavior and highlights the properties of the associated solitary wave.

$$\xi = x - \left(1 - 2v^2\right)t, \quad U_1(\xi) = \pm v\sqrt{\frac{6}{\alpha}}\tanh(\xi). \tag{57}$$

4.2.2 Case 2

We assume that $h_0 = v^2C^2(1-m^2)$, $h_2 = -v^2(2m^2-1)$, and $h_4 = -\frac{v^2m^2}{C^2}$, where C is a nonzero real constant and $0 \le m \le 1$ is the Jacobi elliptic functions modulus. Equation 51 yields the following result:

$$\psi(\xi) = C\,\mathrm{cn}(v\xi, m). \tag{58}$$

The solution of Equation 48 can be expressed as follows, illustrating its structure:

$$U_2(\xi) = \pm vm\sqrt{-\frac{6}{\alpha}}\,\mathrm{cn}(v\xi, m), \quad \omega = 1 + v^2\left(2m^2 - 1\right). \tag{59}$$

As $m \to 1$, the solution is obtained, exposing the limiting behavior of the system and highlighting the features of the associated solitary wave.

$$U_2(\xi) = \pm v\sqrt{-\frac{6}{\alpha}}\,\mathrm{sech}(\xi), \quad \xi = x - \left(1 - v^2\right)t. \tag{60}$$

4.2.3 Case 3

We assume that $h_0 = -v^2C^2(1-m^2)$, $h_2 = v^2(2-m^2)$, and $h_4 = -\frac{v^2}{C^2}$. Equation 51 yields the following results:

$$\psi(\xi) = C\,\mathrm{dn}(v\xi, m). \tag{61}$$

The solution of Equation 48 can be written as follows, providing insight into the behavior of the structure under consideration:

$$U_3(\xi) = \pm v\sqrt{\frac{-6}{\alpha}}\,\mathrm{dn}(v\xi, m), \quad \omega = 1 + v^2\left(2 - m^2\right). \tag{62}$$

As $m \to 1$, the solution is obtained, revealing the system's limiting characteristic and emphasizing the accompanying solitary wave.

$$U_3(\xi) = \pm v\sqrt{\frac{-6}{\alpha}}\,\mathrm{sech}(\xi), \quad \xi = x - \left(1 + v^2\right)t. \tag{63}$$

4.2.4 Case 4

We assume that $h_0 = v^2C^2m^2$, $h_2 = -v^2(1+m^2)$, and $h_4 = \frac{v^2}{C^2}$. Equation 51 yields the following results:

$$\psi(\xi) = C\,\mathrm{ns}(v\xi, m) = \frac{C}{\mathrm{sn}(v\xi, m)}. \tag{64}$$

The solution of Equation 48 can be expressed as follows:

$$\omega = 1 - v^2\left(2 - m^2\right), \quad U_4(\xi) = \pm v\sqrt{\frac{6}{\alpha}}\,\mathrm{ns}(v\xi, m). \tag{65}$$

As $m \to 1$, the solution is determined, showing the system's limiting feature and highlighting the accompanying single wave.

$$\xi = x - \left(1 - v^2\right)t, \quad U_4(\xi) = \pm v\sqrt{\frac{6}{\alpha}}\coth(\xi). \tag{66}$$

4.2.5 Case 5

We assume that $h_0 = -v^2C^2m^2$, $h_2 = v^2(2m^2-1)$, and $h_4 = \frac{v^2(1-m^2)}{C^2}$. Equation 51 yields the following outcomes:

$$\psi(\xi) = C\,\mathrm{nc}(v\xi, m) = \frac{C}{\mathrm{dn}(v\xi, m)}. \tag{67}$$

The solution of Equation 48 can be written as follows:

$$\omega = 1 + v^2\left(2m^2 - 1\right), \quad U_5(\xi) = \pm v\sqrt{\frac{6\left(1-m^2\right)}{\alpha}}\,\mathrm{nc}(v\xi, m). \tag{68}$$

As $m \to 1$, the solution is obtained, revealing the system's limiting characteristic and emphasizing the accompanying single wave.

$$\xi = x - \left(1 - v^2\right)t, \quad U_5(\xi) = \pm v\sqrt{\frac{6}{\alpha}}\sec(\xi). \tag{69}$$

4.2.6 Case 6

We assume that $h_0 = -v^2C^2m^2$, $h_2 = v^2(2-m^2)$, and $h_4 = -\frac{v^2(1-m^2)}{C^2}$. Equation 51 provides the following result:

$$\psi(\xi) = C\,nd(v\xi, m) = \frac{C}{dn(v\xi, m)}. \tag{70}$$

The solution of Equation 48 can be expressed as follows:

$$\omega = 1 + v^2\left(2 - m^2\right), \quad U_6(\xi) = \pm v\sqrt{\frac{-6\left(1-m^2\right)}{\alpha}}\;\; nd(v\xi, m). \tag{71}$$

4.2.7 Case 7

We assume that $h_0 = v^2C^2$, $h_2 = v^2(2-m^2)$, and $h_4 = \frac{v^2(1-m^2)}{C^2}$. Equation 51 yields the following result:

$$\psi(\xi) = C\,sc(v\xi, m) = \frac{C\,sn(v\xi, m)}{cn(v\xi, m)}. \tag{72}$$

The solution of Equation 48 can be written as follows:

$$\omega = 1 + v^2\left(2 - m^2\right), \quad U_7(\xi) = \pm v\sqrt{\frac{6\left(1-m^2\right)}{\alpha}}\;\; sc(v\xi, m). \tag{73}$$

As $m \to 0$, the solution is obtained, revealing the system's limiting characteristic and emphasizing the accompanying single wave.

$$\xi = x - \left(1 + 2v^2\right)t, \quad U_7(\xi) = \pm v\sqrt{\frac{6}{\alpha}}\;\; \tan(\xi). \tag{74}$$

4.2.8 Case 8

We consider that $h_0 = v^2C^2$, $h_2 = v^2(2m^2-1)$, and $h_4 = -\frac{v^2m^2(1-m^2)}{C^2}$. Equation 51 yields the following outcomes:

$$\psi(\xi) = C\,sd(v\xi, m) = \frac{C\,sn(v\xi, m)}{dn(v\xi, m)}. \tag{75}$$

The solution of Equation 48 can be written as follows:

$$\omega = 1 + v^2\left(2m^2 - 1\right), U_8(\xi) = \pm vm\sqrt{\frac{6\left(1-m^2\right)}{\alpha}}\;\; sd(v\xi, m). \tag{76}$$

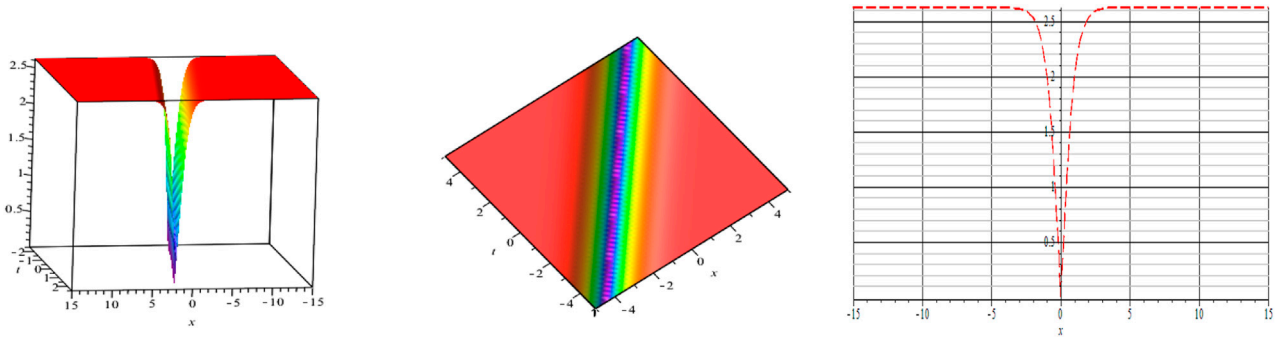

FIGURE 8
Three different graphical representations, namely, 3D surface (left panel), contour plot (middle panel), and 2D profile (right panel), of the solution of Equation 57 for the parameter values $v = 1.3, \alpha = 0.2$. These graphs describe the dark optical soliton under the specified constraints.

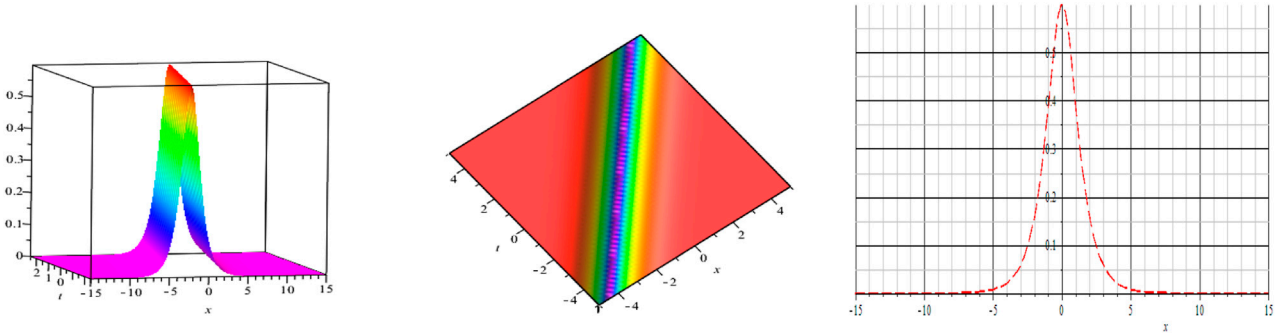

FIGURE 9
Three different graphical representations, namely, 3D surface (left panel), contour plot (middle panel), and 2D profile (right panel), of the solution of Equation 60 for the parameter values $\alpha = 0.8; v = 0.02$. These graphs describe the bright optical soliton under the specified constraints.

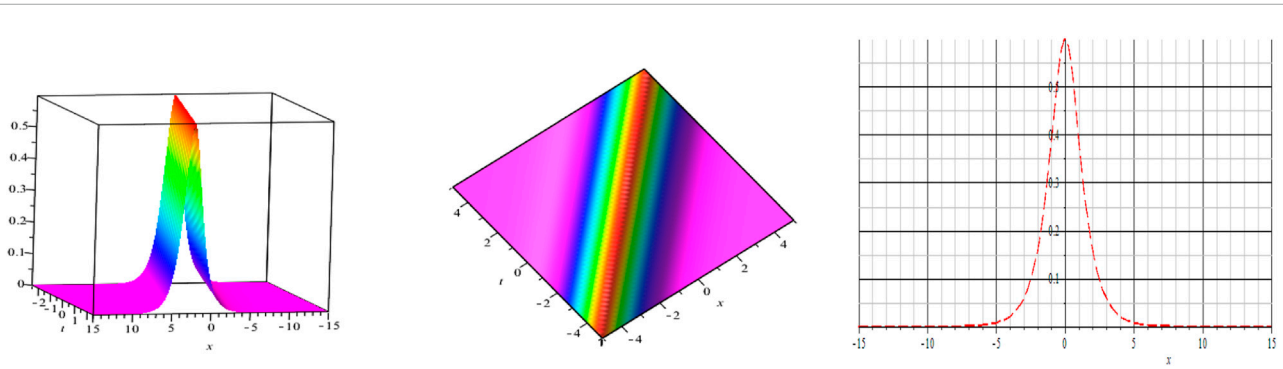

FIGURE 10
Three different graphical representations, namely, 3D surface (left panel), contour plot (middle panel), and 2D profile (right panel), of the solution of Equation 63 for the parameter values $\alpha = 0.8; v = 0.02$. These graphs describe the bright optical soliton under the specified constraints.

4.2.9 Case 9

We consider the equations $h_0 = v^2(1-m^2)C^2$, $h_2 = v^2(2-m^2)$, and $h_4 = \frac{v^2}{C^2}$. Equation 51 yields the following results:

$$\psi(\xi) = C\,cs(v\xi, m) = \frac{C\,cn(v\xi, m)}{sn(v\xi, m)}. \tag{77}$$

The solution of Equation 48 can be written as follows:

$$U_9(\xi) = \pm v\sqrt{\frac{6}{\alpha}}\quad cs(v\xi, m), \quad \omega = 1 + v^2\left(2 - m^2\right). \tag{78}$$

As $m \to 1$, the solution is obtained, showing the system's limiting feature and highlighting the resulting solitary wave.

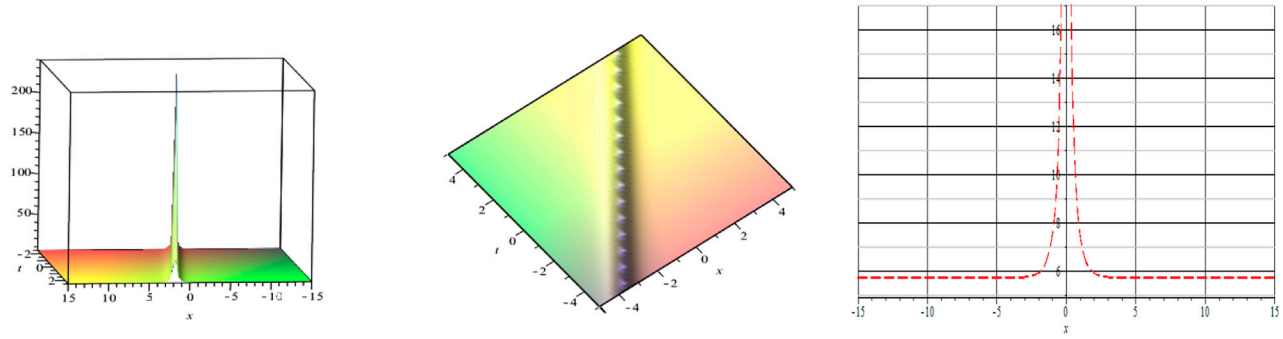

FIGURE 11
Three different graphical representations, namely, 3D surface (left panel), contour plot (middle panel), and 2D profile (right panel), of the solution of Equation 66 for the parameter values $\alpha = 0.01; v = 0.5$. These graphs describe the singular optical soliton under the specified constraints.

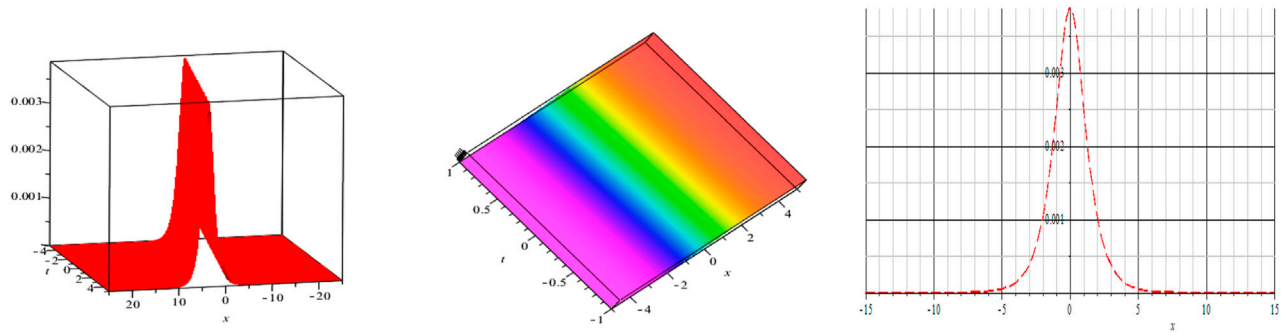

FIGURE 12
Three different graphical representations, namely, 3D surface (left panel), contour plot (middle panel), and 2D profile (right panel), of the solution of Equation 79 for the parameter values $\alpha = 0.001; v = 0.3$. These graphs describe the periodic singular soliton under the specified constraints.

$$\xi = x - (1 + 2v^2)t, \quad U_9(\xi) = \pm v\sqrt{\frac{6}{\alpha}} \quad \cosh(\xi). \tag{79}$$

4.2.10 Case 10

We assume that $h_0 = v^2C^2$, $h_2 = -v^2(1 + m^2)$, and $h_4 = \frac{v^2}{C^2}$. Equation 51 yields the following outcomes:

$$\psi(\xi) = Ccd(v\xi, m) = \frac{Ccn(v\xi, m)}{dn(v\xi, m)}. \tag{80}$$

The solution of Equation 48 can be written as follows:

$$\omega = 1 - v^2(m^2 + 1), U_{10}(\xi) = \pm vm\sqrt{\frac{6}{\alpha}} \quad cd(v\xi, m). \tag{81}$$

4.2.11 Case 11

We consider the following equations $h_0 = -v^2m^2(1 - m^2)C^2$, $h_2 = v^2(2m^2 - 1)$, and $h_4 = \frac{v^2}{C^2}$. Equation 51 yields the following expression:

$$\psi(\xi) = Cds(v\xi, m) = \frac{Cdn(v\xi, m)}{sn(v\xi, m)}. \tag{82}$$

The result of Equation 48 can be written as follows, providing insight into the system's behavior under the provided analysis:

$$\omega = 1 + v^2(2m^2 - 1), \quad U_{11}(\xi) = \pm v\sqrt{\frac{6}{\alpha}} \quad ds(v\xi, m). \tag{83}$$

As $m \to 0$, the solution is obtained, showing the system's limiting feature and emphasizing the associated solitary wave.

$$\xi = x - (1 - v^2)t, \quad U_{11}(\xi) = \pm v\sqrt{\frac{6}{\alpha}} \quad \cosh(\xi). \tag{84}$$

4.2.12 Case 12

We assume that $h_0 = v^2m^2C^2$, $h_2 = -v^2(m^2 + 1)$, and $h_4 = \frac{v^2}{C^2}$. Equation 51 yields the following results:

$$\psi(\xi) = Cdc(v\xi, m) = \frac{Cdn(v\xi, m)}{sn(v\xi, m)}. \tag{85}$$

The solution of Equation 48 can be written as follows:

$$U_{12}(\xi) = \pm v\sqrt{\frac{6}{\alpha}} \quad dc(v\xi, m), \quad \omega = 1 - v^2(m^2 + 1). \tag{86}$$

Table 2 offers a comparative analysis between classical analytical techniques and the more contemporary SMCH and BBM solution families. This comparison highlights the relative advantages and methodological developments within the field.

TABLE 2 Comparison of classical methods with SMCH and BBM solution families.

References	Typical solution in the literature	Computed general solution form	New/improved feature
[46]	Hyperbolic (tanh and sech) and trigonometric solutions (SMCH)	SMCH: U_1, U_2, and U_3 (*tanh*/*sech* variants), U_4 (*coth*), and U_9/U_{11} (*csch*)	More generalized amplitude and velocity parameters; can reduce to classical MSE solutions; allows wider parametric control
[47]	Hyperbolic (*kink*/*tanh*) and trigonometric (*tan*) (SMCH)	SMCH: U_1 and U_{12} (hyperbolic, trigonometric, and elliptic)	Unified hyperbolic, trig, and elliptic forms with explicit parameter constraints; reduction to known results possible
[48]	Solitary waves, periodic waves, and some singular solutions (SMCH)	SMCH: U_1 and U_{12} including elliptic, singular, and periodic	Complete catalog; allows direct comparison and limiting cases; more physical scenarios
[49]	Bright, dark solitons (SMCH)	SMCH: Jacobi elliptic (nd, sd, cd, and ds) and hyperbolic/rational	Adds elliptic families; demonstrates limiting behavior $m \to 0$ (trig) and $m \to 1$ (hyperbolic); unifies periodic and solitary solutions
[50]	Kink, singular, and trigonometric solitons (fractional SMCH)	SMCH: Integer-order, U_1, U_{12} hyperbolic/trig/elliptic with parameter relations	Richer forms than fractional models; amplitude and velocity relations explicitly provided
[51]	Solitary waves (*sech*, *tanh*, abd rational) for BBM	BBM: U_1, U_{12} (sech, tanh, coth, sec, and csch; Jacobi elliptic: nd, sd, cd, and ds)	Unified expressions reducing to standard BBM solutions; explicit parametric dependence; both hyperbolic and elliptic solutions in one framework
[52]	Bright/dark solitons, Jacobi elliptic, and periodic and rational (BBM)	BBM: U_6, U_{12} (Jacobi elliptic: nd, sd, cd, and ds)	Parameter-dependent dispersion relations; limiting checks for $m \to 0$ and $m \to 1$; allows reduction to classical solitary or periodic waves
[53]	Hyperbolic, trigonometric, and rational solutions (BBM)	BBM: U_1, U_5 (tanh, sech, coth, sec, and csch)	More explicit velocity and amplitude parameters; singular forms included; generalization beyond usual G'/G outputs

5 Physical interpretation of solutions under the BBM equation

In this section, the sub-ODE method is used to derive an array of analytical solutions with varying degrees of accuracy for the BBM equation, which is a fundamental model for long-wave propagation in nonlinear dispersive media. The solutions thus obtained are interpreted through the creation of 3D, 2D, and contour plots in Maple 18, which serve to display their dynamic features. A dark soliton solution obtained from Equation 57 is depicted in Figure 8, where the values of the parameters $\nu = 1.3$ and $\alpha = 0.2$ are provided. This wave can be observed as a stable reduction in intensity over the continuous background, which physically corresponds to the context of either a density void or a wave of depression that can be represented in terms of shallow-water waves or plasma physics. The velocity parameter ν and the nonlinear coefficient α determine the soliton's speed and the depth of the trough in the intensity profile, respectively. On the other hand, Figures 9, 10 show the bright soliton solutions from Equations 60, 63, respectively. The solutions are represented as particles or oscillating humps of energy, with $\alpha = 0.8$ and $\nu = 0.02$, and $\alpha = 0.8$ and $\nu = 0.2$, respectively. The difference in the velocity parameter between the figures is ν, and this provides an opportunity for comparing how the speed of propagation affects the amplitude and width of the bright, stable pulses. These pulses are ubiquitous in optical fiber communications and hydrodynamics.

Furthermore, the investigation into the BBM equation reveals that solutions with richer topological features may also be supported. Figure 11 illustrates a singular soliton solution from Equation 66, with parameters $\alpha = 0.01$ and $\nu = 0.5$. This solution comprises a sharp, unbounded peak that is indicative of a wave-breaking scenario or, in other words, the formation of a shock-like structure within a dissipativeless medium. The strong nonlinearity of the solution due to the much smaller value of α compared with the dispersion expresses itself as this steep, singular profile. Complementary to the above, Figure 12 illustrates a periodic singular soliton solution from Equation 79 for $\alpha = 0.001$ and $\nu = 0.3$. The intriguing wave structure involves a periodic recurrence of singularities, suggesting a regime of coherent, repeating blow-up events, which could model phenomena in driven nonlinear lattices

TABLE 3 Summary of soliton solutions and stability analysis.

Figure	Equation	Soliton type	Parameter	Stability	Visual summary
Figure 1	Equation 16	Dark optical	$v = 1.5, j = 1$ $\alpha = 0.1$, and $\beta = 0.5$	Stable	Stable intensity dip, observable in optical fibers
Figure 2	Equation 19	Bright	$v = 1.5, j = 1$ $\alpha = 0.1$, and $\beta = 0.5$ $\chi = 0.1$	Stable	Localized intensity peak, robust against disturbances
Figure 3	Equation 22	Bright optical	$v = 1.5, j = 1$ $\alpha = 0.1$, and $\beta = 0.5$	Stable	Bright pulse, viable for energy transport
Figure 4	Equation 25	Unique structure	$v = 1.5, j = 0$ $\alpha = 0.1$, and $\beta = 0.5$	Conditional	Distinct wave structure, sensitive to parameter j
Figure 5	Equation 28	Periodic singular	$v = 1.5, j = 0$ $\alpha = 0.1$, and $\beta = 0.5$	Unstable	Repeating singularities, blow-up behavior
Figure 6	Equation 33	Periodic	$v = 1.5, j = 0$ $\alpha = 0.1$, and $\beta = 0.5$	Stable	Regular repeating pattern, stable oscillations
Figure 7	Equation 38	Singular optical	$v = 1.5, j = 1$ $\alpha = 0.1$, and $\beta = 0.5$	Unstable	Sharp unbounded peak, inherent instability
Figure 8	Equation 57	Dark optical	$v = 1.3$ and $\alpha = 0.2$	Stable	Stable dark pulse, confirmed eigenvalues
Figure 8	Equation 60	Bright optical	$\alpha = 0.8$ and $v = 0.02$	Stable	Bright pulse, robust stability
Figure 9	Equation 63	Bright optical	$\alpha = 0.8$, $v = 0.2$	Stable	Bright soliton, stable at higher velocity
Figure 10	Equation 66	Singular optical	$\alpha = 0.01$ and $v = 0.5$	Unstable	Singular structure, exponential growth
Figure 11	Equation 79	Periodic singular	$\alpha = 0.001$ and $v = 0.3$	Unstable	Periodic singularities, divergent response

or certain unstable wave regimes. Regarding the development of each solution, the parameters were carefully chosen in order to ensure numerical stability and definitely isolate each type of soliton.

The comprehensive graphical representation, systematically presenting the 3D, 2D, and contour plots for each solution, offers a multifaceted analysis of the wave dynamics inherent to the BBM equation. Each 3D surface plot allows for a vivid depiction of the temporal evolution and robust spatial localization of each soliton, thereby demonstrating their stability during propagation. Corresponding 2D line graphs provide an exact cross-section view of the instantaneous amplitude profile of the wave, allowing one to compare waveforms such as dark depression and bright peak clearly. Finally, the contour plots map the propagation pathways and regions of energy concentration, providing insight into the wave's interaction potential and dispersive properties. The BBM equation's ability to model complex wave phenomena in dispersive media is substantiated by the diverse range of wave morphologies, which are not merely dark and bright but also singular and periodic, which the equation supports. The importance of the BBM equation is thus reaffirmed through the use of these visualizations, which not only illustrate mathematical functions but also confirm the existence of wave morphologies that are very varied in nature.

This work systematically classifies its contributions to clearly delineate their novelty against established literature. Our results include solutions matching classical solitons, such as the standard bright (*sech*-type) and dark (*tanh*-type) solitary waves, which serve to validate our methods through the recovery of known results. Importantly, we generalized several known families by deriving solutions with extended parametric pre-factors, such as a velocity-dependent scaling in the periodic *tan*-type solution, allowing enhanced control over the soliton dynamics. The core novelty, however, is in the new solutions reported herein, which are inclusive of the *sec*-type singular solution U_5 and the suite of previously unreported Jacobi elliptic solutions $U_6, U_8, U_{10}, U_{11}, U_{12}$ with fully specified dispersion relations. Critical demonstration of their validity and generality is also derived from their correct reduction to known classical limits; in other words, as the modulus $m \to 1$, the elliptic solutions here correctly reduce to hyperbolic *sech*/*tanh* solitons, and as $m \to 0$, they simplify into trigonometric periodic waves. Hence, this work extends the known landscape of analytical solutions, offering both a broader unifying framework and specific, novel waveforms for future application. Table 3 summarizes the obtained soliton solutions and provides a dedicated assessment of their stability. So, this table present a consolidated view of both the derived solution sand their dynamical robustness.

6 Conclusion

In this study, the sub-ODE method is effectively used to derive and analyze several forms of soliton solutions for the nonlinear SMCH and BBM equations. New traveling wave solutions involving hyperbolic, exponential, and trigonometric functions have been obtained for these nonlinear models. This approach is well-structured and effective for producing analytical solutions to nonlinear partial differential equations. Specific 3D, 2D, and contour graphs are used to illustrate the physical behaviors of the SMCH and BBM equations using Maple 18. The exact solutions obtained include dark, bright, single, and periodic solitons. Both the SMCH and BBM equations are important in the study of nonlinear wave propagation as they provide insight into the behavior of solitons in a variety of physical systems. By studying these equations and their solutions, researchers can gain a deeper understanding of fundamental nonlinear phenomena and develop

innovative technologies that use soliton properties. These solutions are extremely useful, with extensive applications in engineering, optical fibers, applied mathematics, and nuclear physics.

The present work has successfully advanced the field of nonlinear wave dynamics by systematically deducing a wide spectrum of new analytical soliton solutions for two key model equations. The key novelty of the results presented lies not only in the application of the sub-ODE method to derive such solutions but also in the comprehensive characterization of their stability—a crucial step that is often overlooked in similar analytical studies. We have moved beyond simple solution generation and provided a comprehensive physical classification, confirming the existence of stable bright and dark solitons, which are essential in optical communication systems, while also identifying and simultaneously for determining unstable and singular structures that define the operation limits of such systems. The clear link drawn between specific ranges of the parameters and soliton stability is a significant contribution, providing a practical roadmap through which experimentalists can achieve these waveforms in laboratory conditions. The discovery of unique, conditionally stable soliton structures will further expand the known catalog of waveforms and suggest new directions for theoretical investigation. This work incorporates detailed visual analytics with rigorous stability criteria, hence bridging an important gap between abstract mathematical solutions and tangible physical applicability, strongly positioning our findings as a meaningful and predictive contribution to the ongoing research within the context of integrable systems and applied mathematical physics.

Data availability statement

The raw data supporting the conclusions of this article will be made available by the authors, without undue reservation.

Author contributions

TZ: Conceptualization, Data curation, Formal Analysis, Funding acquisition, Investigation, Methodology, Project administration, Resources, Software, Supervision, Validation, Visualization, Writing – original draft, Writing – review and editing.

Funding

The author(s) declared that financial support was not received for this work and/or its publication.

Acknowledgements

The author sincerely appreciates the editor and the reviewers for their time, insightful comments, and constructive feedback, which have significantly enhanced the quality of this manuscript.

Conflict of interest

The author(s) declared that this work was conducted in the absence of any commercial or financial relationships that could be construed as a potential conflict of interest.

Generative AI statement

The author(s) declared that generative AI was not used in the creation of this manuscript.

Any alternative text (alt text) provided alongside figures in this article has been generated by Frontiers with the support of artificial intelligence and reasonable efforts have been made to ensure accuracy, including review by the authors wherever possible. If you identify any issues, please contact us.

Publisher's note

References

1. Rosenbluh M, Shelby RM. Squeezed optical solitons. *Phys Review Letters* (1991) 66:153–6. doi:10.1103/PhysRevLett.66.153

2. Liu S, Fu Z, Liu S, Zhao Q. Jacobi elliptic function expansion method and periodic wave solutions of nonlinear wave equations. *Phys Lett A* (2001) 289:69–74. doi:10.1016/S0375-9601(01)00580-1

3. Feng Z. The first-integral method to study the burgers–korteweg–de vries equation. *J Phys A: Math Gen* (2002) 35:343–9. doi:10.1088/0305-4470/35/2/312

4. Zhang SL, Wu B, Lou SY. Painlevé analysis and special solutions of generalized broer–kaup equations. *Phys Lett A* (2002) 300:40–8. doi:10.1016/S0375-9601(02)00688-6

5. Wazwaz AM. The tan h method: solitons and periodic solutions for the dodd–bullough–mikhailov and the Tzitzeica–Dodd–Bullough equations. *Chaos, Solitons and Fractals* (2005) 25:55–63. doi:10.1016/j.chaos.2004.09.122

6. Wazwaz AM. Adomian decomposition method for a reliable treatment of the emden–fowler equation. *Appl Mathematics Comput* (2005) 161:543–60. doi:10.1016/j.amc.2003.12.048

7. Yomba E. The extended Fan's sub-equation method and its application to KdV–MKdV, BKK and variant boussinesq equations. *Phys Lett A* (2005) 336:463–76. doi:10.1016/j.physleta.2005.01.027

8. Zhao X, Wang L, Sun W. The repeated homogeneous balance method and its applications to nonlinear partial differential equations. *Chaos, Solitons and Fractals* (2006) 28:448–53. doi:10.1016/j.chaos.2005.06.001

9. Yusufoğlu E, Bekir A. Solitons and periodic solutions of coupled nonlinear evolution equations by using the sine–cosine method. *Int J Computer Mathematics* (2006) 83:915–24. doi:10.1080/00207160601138756

10. Wazwaz AM. The Hirota's bilinear method and the tanh–coth method for multiple-soliton solutions of the sawada–kotera–kadomtsev–petviashvili equation. *Appl Mathematics Comput* (2008) 200:160–6. doi:10.1016/j.amc.2007.11.001

11. Yusufoğlu E. New solitonary solutions for the MBBM equations using Exp-function method. *Phys Lett A* (2008) 372:442–6. doi:10.1016/j.physleta.2007.07.062

12. Manafian J. Optical soliton solutions for schrödinger type nonlinear evolution equations by the tan(Φ (ξ)/2)-expansion method. *Optik* (2016) 127:4222–45. doi:10.1016/j.ijleo.2016.01.078

13. Kibler B, Fatome J, Finot C, Millot G, Dias F, Genty G, et al. The peregrine soliton in nonlinear fibre optics. *Nat Physics* (2010) 6:790–5. doi:10.1038/nphys1740

14. Maimistov AI. Solitons in nonlinear optics. *Quan Electronics* (2010) 40:756–81. doi:10.1070/QE2010v040n09ABEH014396

15. Mohyud-Din ST, Noor MA, Noor KI. Exp-function method for traveling wave solutions of modified zakharov–kuznetsov equation. *J King Saud University-Science* (2010) 22:213–6. doi:10.1016/j.jksus.2010.04.015

16. Zayed E, Al-Joudi S. Applications of an extended (*G*/*G*)-Expansion method to find exact solutions of nonlinear PDEs in mathematical physics. *Math Probl Eng* (2010) 2010:768573. doi:10.1155/2010/768573

17. Ebadi G, Kara A, Petkovi´c MD, Biswas A. Soliton solutions and conservation laws of the gilson–pickering equation. *Waves in Random and Complex Media* (2011) 21:378–85. doi:10.1080/17455030.2011.569036

18. Wazwaz AM. A new (2 + 1)-dimensional Korteweg–de vries equation and its extension to a new (3+ 1)-dimensional kadomtsev–petviashvili equation. *Physica Scripta* (2011) 84:035010. doi:10.1088/0031-8949/84/03/035010

19. Zayed EM. A note on the modified simple equation method applied to sharma–tasso–olver equation. *Appl Mathematics Comput* (2011) 218:3962–4. doi:10.1016/j.amc.2011.09.025

20. Naher H, Abdullah FA, Akbar MA. New traveling wave solutions of the higher Dimen-sional nonlinear partial differential equation by the exp-function method. *J Appl Mathematics* (2012) 2012:575387. doi:10.1155/2012/575387

21. Bekir A, Güner Ö. Exact solutions of nonlinear fractional differential equations by (*G*/*G*)- expansion method. *Chin Phys B* (2013) 22:110202. doi:10.1088/1674-1056/22/11/110202

22. Alam MN, Akbar MA. The new approach of the generalized (*G*/*G*)-expansion method for nonlinear evolution equations. *Ain Shams Eng J* (2014) 5:595–603. doi:10.1016/j.asej.2013.12.008

23. Zheng B. A new fractional jacobi elliptic equation method for solving fractional partial differential equations. *Adv Difference Equations* (2014) 2014:228. doi:10.1186/1687-1847-2014-228

24. Kilic B, Inc M. Optical solitons for the schrödinger–hirota equation with power law nonlin-earity by the bäcklund transformation. *Optik* (2017) 138:64–7. doi:10.1016/j.ijleo.2017.03.017

25. Islam MN, Akbar MA. New exact wave solutions to the space-time fractional-coupled burgers equations and the space-time fractional foam drainage equation. *Cogent Phys* (2018) 5:1422957. doi:10.1080/23311940.2017.1422957

26. Körpınar T, Demirkol RC, Körpınar Z. Soliton propagation of electromagnetic field vectors of polarized light ray traveling along with coiled optical fiber on the unit 2-sphere *S*2. *Revista Mexicana Def Ísica* (2019) 65:626–33. doi:10.31349/RevMexFis.65.626

27. Wazwaz AM, Kaur L. Optical solitons and Peregrine solitons for nonlinear schrödinger equation by variational iteration method. *Optik* (2019) 179:804–9. doi:10.1016/j.ijleo.2018.11.004

28. Bagri M, Kumar S. Solitons transmission system: a dynamic shift in optical fiber communica-tion. *Indian J Sci Technol* (2020) 13:2193–202. doi:10.17485/IJST/v13i30.384

29. Tanwar DV, Wazwaz AM. Lie symmetries, optimal system and dynamics of exact solutions of (2 + 1)-dimensional KP-BBM equation. *Physica Scripta* (2020) 95:065220. doi:10.1088/1402-4896/ab8651

30. Tanwar DV. Optimal system, symmetry reductions and group-invariant solutions of (2 + 1)-dimensional ZK-BBM equation. *Physica Scripta* (2021) 96:065215. doi:10.1088/1402-4896/abf00a

31. Tanwar DV, Wazwaz AM. Lie symmetries and exact solutions of KdV–Burgers equation with dissipation in dusty plasma. *Qual Theory Dynamical Systems* (2022) 21:164. doi:10.1007/s12346-022-00692-w

32. Tanwar DV, Sahu P. Dynamics of one-dimensional motion of a gas under the influence of monochromatic radiation. *Qual Theor Dynamical Syst* (2023) 22:54. doi:10.1007/s12346-023-00752-9

33. Kumar M, Tanwar DV. On lie symmetries and invariant solutions of (2 + 1)–dimensional gardner equation. *Commun Nonlinear Sci Numer Simulation* (2019) 69:45–57. doi:10.1016/j.cnsns.2018.09.009

34. Tanwar DV, Wazwaz AM. Lie symmetries and dynamics of exact solutions of dissipative zabolotskaya–khokhlov equation in nonlinear acoustics. *The Eur Phys J Plus* (2020) 135:520. doi:10.1140/epjp/s13360-020-00527-0

35. Tanwar DV, Kumar R, Asthana N. Invariant Solutions and Dynamics of Soliton to Coupled Burgers Equations: DV Tanwar et al Qualitative Theory of Dynamical. *Systems* (2025) 24:206. doi:10.1007/s12346-025-01366-z

36. Tanwar DV, Tanwar DV. Lie symmetry reductions and exact solutions of kadomtsev–petviashvili equation. *Pramana* (2025) 99:35. doi:10.1007/s12043-024-02887-z

37. Tanwar DV. On lie symmetries, soliton interaction nature and conservation laws of Broer- kaup-kupershmidt system in shallow water of uniform depth. *Physica Scripta* (2025) 100:025225. doi:10.1088/1402-4896/ada4f8

38. Macia-Castello C, Blanco-Lopez D, Gaboardi M, Koenders E, Dolado JS, Wakabayashi Y, et al. Energy-resolved imaging and tomography with compact neutron Systems—application to novel construction materials for thermal-energy storage. *Can J Phys* (2025) 103:1232–40. doi:10.1139/cjp-2025-0085

39. Ahmad I, Faridi WA, Iqbal M, Majeed Z, Tchier F. Exploration of soliton solutions in nonlinear optics for the third order klein-fock-gordon equation and nonlinear Maccari's system. *Int J Theor Phys* (2024) 63:157. doi:10.1007/s10773-024-05692-x

40. lhan OA, Manafian J, Baskonus HM, Lakestani M. Solitary wave solitons to one model in the shallow water waves. *The Eur Phys J Plus* (2021) 136:337. doi:10.1140/epjp/s13360-021-01327-w

41. Kumar S, Almusawa H, Hamid I, Abdou M. Abundant closed-form solutions and solitonic structures to an integrable fifth-order generalized nonlinear evolution equation in plasma physics. *Results Physics* (2021) 26:104453. doi:10.1016/j.rinp.2021.104453

42. Seadawy AR, Ali A, Althobaiti S, Sayed S. Propagation of wave solutions of nonlinear heisenberg ferromagnetic spin chain and vakhnenko dynamical equations arising in nonlinear water wave models. *Chaos, Solitons and Fractals* (2021) 146:110629. doi:10.1016/j.chaos.2020.110629

43. Shen Y, Tian B, Zhang CR, Tian HY, Liu SH. Breather-wave, periodic-wave and traveling-wave solutions for a (2 + 1)-dimensional extended boiti–leon–manna–pempinelli equation for an incompressible fluid. *Mod Phys Lett B* (2021) 35:2150261. doi:10.1142/S0217984921502614

44. Mohammed F, Elboree MK. Soliton solutions and periodic solutions for two models arises in mathematical physics. *AIMS Math* (2021) 7:4439–58. doi:10.3934/math.2022247

45. Mathanaranjan T, Kumar D, Rezazadeh H, Akinyemi L. Optical solitons in metamaterials with third and fourth order dispersions. *Opt Quan Electronics* (2022) 54:271. doi:10.1007/s11082-022-03656-1

46. Islam MN, Asaduzzaman M, Ali MS. Exact wave solutions to the simplified modified camassa-holm equation in mathematical physics. *Aims Math* (2019) 5:26–41. Available online at: https://li05.tci-thaijo.org/index.php/buuscij/article/view/677 (Accessed October 17, 2019).

47. Sanjun J, Jindayen K, Onrak K. Two methods with the riccati equation to seek traveling wave solutions for the simplified modified camassa-holm equation. *Burapha Sci J* (2025) 30:758–77. Available online at: https://li05.tci-thaijo.org/index.php/buuscij/article/view/677 (Accessed August 8, 2025).

48. Islam SR, Arafat SY, Wang H. Abundant closed-form wave solutions to the simplified modified camassa-holm equation. *J Ocean Engineering Science* (2023) 8:238–45. doi:10.1016/j.joes.2022.01.012

49. Parvin H, Alam MN, Hossain MF, Hassan M, Hossen MJ. Computational study of soliton behavior in the simplified modified form of the camassa-holm equation. *Aims Mathe.* (2025) 10:21533–48. doi:10.3934/math.2025957

50. Onder I, Cinar M, Secer A, Bayram M. Analytical solutions of simplified modified Camassa- holm equation with conformable and M-truncated derivatives: a comparative study. *J Ocean Engineering Science* (2024) 9:240–50. doi:10.1016/j.joes.2022.06.012

51. Tariq KU, Seadawy AR. On the soliton solutions to the modified benjamin-bona-mahony and coupled Drinfel'd-Sokolov-Wilson models and its applications. *J King Saud University- Sci* (2020) 32:156–62. doi:10.1016/j.jksus.2018.03.019

52. Yasmin H, Alyousef HA, Asad S, Khan I, Matoog R, El-Tantawy S. The riccati-bernoulli sub-optimal differential equation method for analyzing the fractional dullin-gottwald-holm equation and modeling nonlinear waves in fluid mediums. *AIMS Mathematics* (2024) 9:16146–67. doi:10.3934/math.2024781

53. Latif M The improved (G'/G)-expansion method is equivalent to the tanh method. arXiv preprint arXiv:1506.06025 2015. doi:10.48550/arXiv.1506.06025